

High-Sensitivity Stark Spectroscopy Obtained by Surface Plasmon Resonance Measurement

S. Wang, S. Boussaad, S. Wong, and N. J. Tao*

Department of Physics, Florida International University, Miami, Florida 33199

The effect (Stark effect) of an applied electric field on the electronic states of molecular adsorbates was studied by measuring surface plasmon resonance (SPR) as a function of the wavelength of the incident light that excites the SPR. Using the Kramers–Kronig relation, Stark spectra comparable to those obtained with conventional methods were extracted from the electric field-induced SPR angular shift for several organic adsorbates. Because this method relies on detecting the SPR angular shift that can be measured precisely, high-sensitivity Stark spectroscopy can be achieved. In addition, the adsorbate coverage information can be determined from the SPR angular shift upon molecular adsorption.

The effect of an applied electric field on the absorption or emission spectra of molecules is known as the Stark effect. Stark spectroscopy measures the Stark effect by measuring the change in the absorption spectra of molecules as the applied field is changed. The technique has been used to study a wide range of molecular systems and materials. The principle, methodology, and applications of Stark spectroscopy are well documented in literature.¹ A typical Stark spectroscopy measurement involves working with frozen samples, which is not desirable for many temperature-sensitive samples such as biological samples. Alternative methods that avoid lowering the sample temperature include Langmuir–Blodgett (LB) films² and the self-assembled monolayer (SAM).³ The preparation of LB film requires a Langmuir trough with deposition device and amphiphilic molecules. The preparation of a SAM is a simpler task. However, because the SAM is only a single molecular layer, the ability to measure a small amount of light absorption is required in order to obtain the Stark spectroscopy using conventional methods.

Potential-modulated UV–visible electroreflectance absorption spectroscopy has been used to measure Stark spectroscopy.^{4–8}

In the method, sample molecules are adsorbed or self-assembled onto an electrode surface and the electric field at the electrode–electrolyte interface is changed by modulating the electrochemical potential of the electrode. The reflectance change caused by the potential modulation as a function of the incident light wavelength is usually measured with a lock-in amplifier. In the absence of potential-induced electrochemical processes, such as reactions and adsorption/desorption, the reflectance change measures the Stark effect. The ultimate sensitivity of the electroreflectance-based technique is determined by how small a change in the reflectance can be measured. Because electroreflectance involves light passing through the bulk solution, it is necessary to separate potential-induced changes in the molecules adsorbed on the surface from those in the bulk solution.^{6–8}

Surface plasmon resonance (SPR) has emerged as a powerful technique for a variety of chemical and biological sensor applications.^{9–16} Surface plasmons are collective oscillations of free electrons in a metallic film. Under the appropriate conditions, the plasmons can be set to resonate with light, which results in the absorption of light.^{17,18} Because the resonant condition is extremely sensitive to the refractive index of the medium adjacent to the metal film, adsorption of molecules on the metallic film or conformational changes in the adsorbed molecules can be accurately detected. Peterlinz and Georgiadis used two-color SPR to obtain the thickness of adsorbed molecular layers.¹⁹ We recently reported a multicolor angle-resolved SPR setup that has capability of measuring the electronic states of the molecules.²⁰ We present here a novel approach to obtain Stark spectroscopy for molecular adsorbates using high-resolution SPR.²¹ This approach provides high-sensitivity Stark spectroscopy with little interference from molecules in bulk solution and additional information about adsorption kinetics and adsorbate coverage.

* Corresponding author: (e-mail) taon@fiu.edu.

- (1) Bublitz, G. U.; Boxer, S. G. *Annu. Rev. Phys. Chem.* **1997**, *48*, 213–242.
- (2) Ohta, N.; Okazaki, S.; Yamazaki, I. *Chem. Phys. Lett.* **1994**, *229*, 394–400.
- (3) Lezna, R. O.; Juanto, S.; Zagal, J. H. *J. Electroanal. Chem.* **1995**, *389*, 197–200.
- (4) Satoshi, T.; Igarashi, S.; Sato, H.; Niki, K. *Langmuir* **1991**, *7*, 1005–1012 and the references therein.
- (5) Ngameni, E.; Laouéna A.; L'Her, M. *J. Electroanal. Chem.* **1991**, *301*, 207–226.
- (6) Sagara, T.; Niki, K. *Langmuir* **1993**, *9*, 831–838.
- (7) Sagara, T.; Takagi, S.; Niki, K. *J. Electroanal. Chem.* **1993**, *349*, 159–171.
- (8) Sagara, T.; Wang, H. X.; Niki, K. *J. Electroanal. Chem.* **1994**, *364*, 285–288.

- (9) Fisher, R. J.; Fivash, M. *Curr. Biotechnol.* **1994**, *45*, 65–71.
- (10) Frutos, A. G.; Corn, R. M. *Anal. Chem.* **1998**, *70*, 449A–455A.
- (11) Homola, J.; Yee, S. S.; Gauglitz, G. *Sens. Actuators B* **1999**, *54*, 3–15.
- (12) Nylander, C.; Liedberg, B.; Lind, T. *Sens. Actuators* **1982**, *3*, 79–88.
- (13) Nrktsich, M.; Sigal, G. B.; Whitesides, G. M. *Langmuir* **1995**, *11*, 4383–4385.
- (14) Sota, H.; Hasegawa, Y.; Iwakura, M. *Anal. Chem.* **1998**, *70*, 2019–2024.
- (15) Salamon, Z.; Wang, Y.; Tollin, G. *Biophys. J.* **1996**, *71*, 283–289.
- (16) Haussling, L.; Ringsdorf, H.; Schmitt, F.-J.; Knoll, W. *Langmuir* **1991**, *7*, 1837–1840.
- (17) Otto, A. *Z. Phys.* **1968**, *216*, 398–407.
- (18) Kretschmann, E. *Z. Phys.* **1971**, *241*, 313–324.
- (19) Peterlinz, K. A.; Georgiadis, R. *Opt. Commun.* **1996**, *130*, 260–266.
- (20) Boussaad, S.; Pean, J.; Tao, N. J. *Anal. Chem.* **2000**, *72*, 222–226.
- (21) Tao, N. J.; Boussaad, S.; Huang, W. L.; Arechabaleta, R. A.; D'Agnesse, J. *Rev. Sci. Instrum.* **1999**, *70*, 4656–4660.

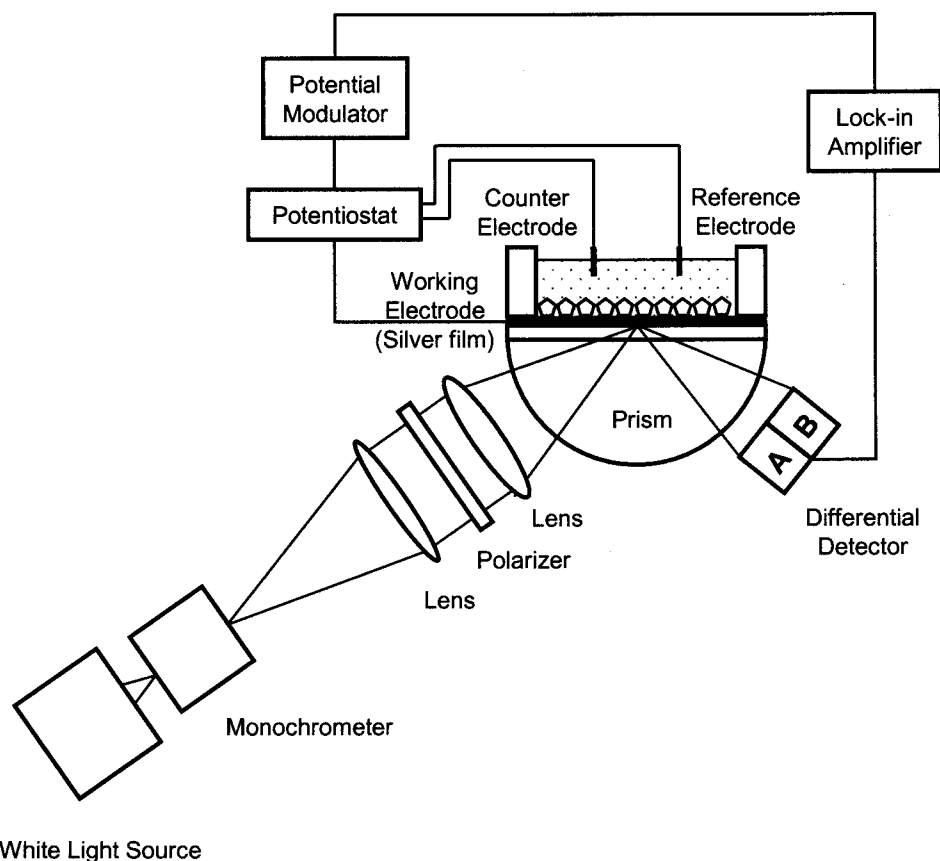


Figure 1. Schematic of the SPR-based Stark spectroscopy setup.

PRINCIPLE

The most widely used SPR methods are based on attenuated total internal reflection in a prism on which a thin metal film is coated.^{17,18} In the methods, p-polarized light is incident upon the metal film and its reflection is detected (Figure 1). When the angle of the incident light reaches an appropriate value, the reflection decreases sharply to a minimum, corresponding to the resonance of surface plasmons in the film.

In the absence of electrochemical reactions, adsorption or desorption, a small modulation in the electrode potential (ΔV) can shift the resonant angle ($\Delta\theta$), via changes in the refractive index (Δn), average thickness (Δd) of the adsorbed molecular layer, and surface charge density ($\Delta\sigma$) of the electrode. The potential-induced shift is given by

$$\frac{\Delta\theta(\lambda)}{\Delta V} = c_1 \frac{\Delta n(\lambda)}{\Delta V} + c_2 \frac{\Delta d}{\Delta V} + c_3 \frac{\Delta\sigma}{\Delta V} \quad (1)$$

where c_1 , c_2 , and c_3 are constants and λ is the wavelength of the incident light.

The first term in eq 1 describes changes in the electronic states of the adsorbed molecules upon modulation of the electrode potential, which can arise from the Stark effect. Knowing $\Delta\theta/\Delta V$ vs λ , the change in the molar extinction coefficient ($\Delta\epsilon$) as measured by conventional Stark spectroscopy can be obtained according to the Kramers–Kronig relation,²²

$$\frac{\Delta\epsilon(\lambda)}{\Delta V} \sim -\frac{2\lambda}{\pi} P \int_0^\infty \frac{(\Delta\theta(\lambda')/\Delta V)}{\lambda'^2 - \lambda^2} d\lambda' \quad (2)$$

where P in front of the integral sign implies how the infinity at $\lambda' = \lambda$ should be treated. The upper limit of the integral is infinite, but the relation can still provide an accurate result in practice even if data are available over only a limited wavelength range.²³ When λ is far away from any absorption band, this term measures the electric field-induced changes in the index of refraction, or the electrooptic properties of the molecules. In a recent novel application of potential-modulated SPR, Hanken and Corn were able to extract the electric field profile inside the multilayer film of zirconium phosphonate, a noncentrosymmetric molecule with a known electrooptic coefficient.²⁴

The second term describes the change of the thickness of the molecular layer upon modulation of the electrode potential, which is a piezoelectric effect and usually a constant for a small potential modulation. The third term can be traced to the dependence of the surface plasmon resonant frequency on the surface charge density.²⁵ This term is proportional to the surface capacitance that varies as $1/d$. Both the second and third terms are λ independent; therefore, they do not affect the Stark spectroscopy.

If there is no optical absorption within the measured wavelength range, the first term is also wavelength independent and eq 1 is reduced to

(22) Kittel, C. *Solid State Physics*; John Wiley & Sons: New York, 1996.

(23) Cantor, C. R.; Schimmel, P. R. *Biophysical Chemistry, Part II: Techniques for the study of biological structure and function*; W. H. Freeman and Co.: New York, 1980.

(24) Hanken, D. G.; Corn, R. M. *Anal. Chem.* **1997**, *69*, 3665–3673.

(25) Kotz, R.; Kolb, D. M.; Sass, J. K. *Surf. Sci.* **1977**, *69*, 359–364.

$$\frac{\Delta\theta(\lambda)}{\Delta V} \propto \text{const} + \frac{1}{d} \quad (3)$$

MATERIALS AND METHODS

Instrumentation. The SPR setup used a BK7 planocylindrical lens (Melles Griot) as prism. On the prism, a BK7 glass slide, coated with a 45-nm-thick silver or gold film by a sputtering coater, was placed with an index matching fluid. White light from a 150-W xenon lamp (Oriel) was sent to a monochromator. Monochromatic light with a bandwidth of ~ 0.5 nm from the monochromator was collimated and then focused by a 14-mm focal-length lens through the prism onto the silver film. Light reflected from the silver film was detected with a bicell photodiode detector (Hamamatsu Corp., model S2721-02), which was mounted on a precision translation stage. In each measurement, the prism was rotated such that a dark line, corresponding to the SPR dip, was located at the center of the laser beam. The reflected light falling onto the two cells of the photodetector was then balanced by adjusting the photodetector position with the translation stage until the differential signal approached zero. A shift in SPR angle is proportional to the differential angle, which can be precisely measured.²¹ The response of the differential signal to the modulation of the electrode potential as a function of λ was recorded with a lock-in amplifier (Princeton Applied Research, model 5110). The output from the lock-in amplifier normalized by the sum signal of the photodetector is proportional to $\Delta\theta(\lambda)/\Delta V$, which was used to calculate Stark spectrum, $\Delta\epsilon/\Delta V$, according to eq 2.

A Teflon sample cell was mounted on the silver film to hold sample solutions. To control the electrode potential, Pt and Ag wires were used as counter and quasi-reference electrodes, respectively, with a potentiostat (Pine Instruments). The quasi-reference electrode was calibrated, and the potential is quoted in this paper with respect to an Ag/AgCl (in 3 M KCl) reference electrode. The experiments were conducted with the electrode being held at 0.2 V while a ± 10 mV modulation at 200 Hz was applied to the potential. The potential was chosen such that no electrochemical reactions taking place on the silver film.

In situ STM experiments were carried out on a Pico STM (Molecular Imaging Co.) using a bias voltage of 0.1 V and a tunneling current of 100 pA. The STM tips were etched electrochemically in 10 M NaOH from 0.25-mm-diameter Pt_{0.8}Ir_{0.2} wires and then coated with Apiezon wax. Gold substrates were grown epitaxially on mica under ultrahigh vacuum (UHV) conditions and stored in a chamber filled with argon gas. Each substrate was briefly flamed with a H₂ torch before each experiment. Immediately after annealing, the substrate was mounted into a homemade Teflon STM cell or SPR cell and covered with the sample solution.

Chemicals. Sodium perchlorate, sodium phosphate, methylene blue, and thiol molecules (HS(CH₂)_nCH₃) with different lengths were purchased from Sigma-Aldrich. Transition metal phthalocynine–tetrasulfonic acid tetrasodium salts (Ni, Zn, and Fe) are purchased from Porphyrin Products, Inc. (Logan, UT). They were used without further purification.

RESULTS

To verify the basic concept presented in the Principle section, we have chosen two types of molecules: alkanethiols and dye

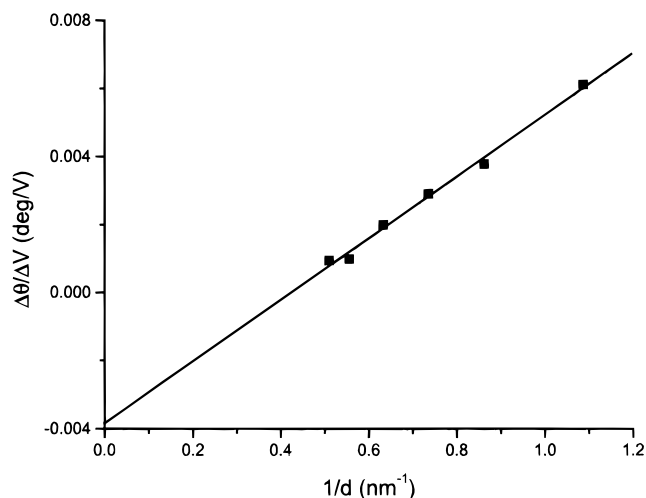


Figure 2. Potential-induced SPR angular shift of thiol SAMs (C_nH_{2n+1}SH, $n = 8, 10, 12, 14, 16, 18$) on silver film as a function of thickness. Potential: 0.2 V, modulation ± 10 mV, 200 Hz.

molecules. The former has no Stark effect because the thiol molecules absorb no light in the visible range. Alkanethiols are well known to self-assemble onto silver or gold surfaces and form a well-defined monolayer. By varying the chain length of the molecules, the thickness of the monolayer can be easily varied. These features make alkanethiols ideal for testing the second and third terms in eq 1. The dye molecules that we choose are transition metal phthalocynine–tetrasulfonic acid tetrasodium salts and methylene blue. These molecules have pronounced absorption peaks in the visible range, which should lead to the Stark effect described by the first term of eq 1.

Surface Charge and Molecular Thickness Effects. Thiol molecules (HS(CH₂)_nCH₃, $n = 8, 10, 12, 14, 16, 18$) were self-assembled onto the silver electrodes by exposing each electrode to 1 mM thiol dissolved in ethanol. The thiol-coated electrode was then mounted in the SPR solution cell and covered with 0.1 M NaClO₄ electrolyte. For a given wavelength ($\lambda = 670$ nm), the measured $\Delta\theta/\Delta V$ was plotted as a function of $1/d$ in Figure 2, where d , the thickness of thiol layer, was calculated from the chain length of each thiol molecule with a software (CS Chem3d Pro). Previous experiments have shown that the thickness of self-assembled thiol layer is linearly proportional to the chain length.²⁶ The SPR angular shift in response to the potential modulation is linearly proportional to $1/d$, as shown in Figure 2. This result is in good agreement with the prediction by eq 3. The linear curve intercepts the vertical axis at $\sim -0.004^\circ/\text{V}$. Assuming the $0.004^\circ/\text{V}$ offset is purely from the second term in eq 1, the piezo constant, $\Delta d/\Delta V$, is estimated to be ~ 0.01 nm/V. A precise analysis of this term, however, requires a good understanding of the double-layer structure, as well as the dependence of the Ag–S bonding on the electrode potential.

Stark Effect. We studied Stark spectroscopy of Ni(II)– and Zn–phthalocynine–tetrasulfonic acid tetrasodium salts (as NiPh and ZnPh below) and methylene blue with the SPR method. We started each experiment by measuring the SPR response ($\Delta\theta/\Delta V$) in blank NaClO₄ as a function of λ . We then introduced a

(26) Zhang, Y.; Terrill, R. H.; Bohn, P. W. *J. Am. Chem. Soc.* **1998**, *120*, 9969–9970.

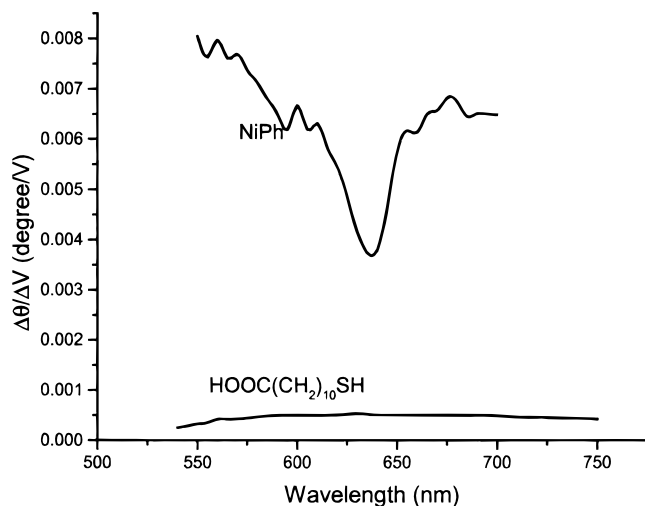


Figure 3. Potential-induced SPR angular shift of $\text{HOOC}(\text{CH}_2)_{10}\text{SH}$ and NiPh as a function of wavelength.

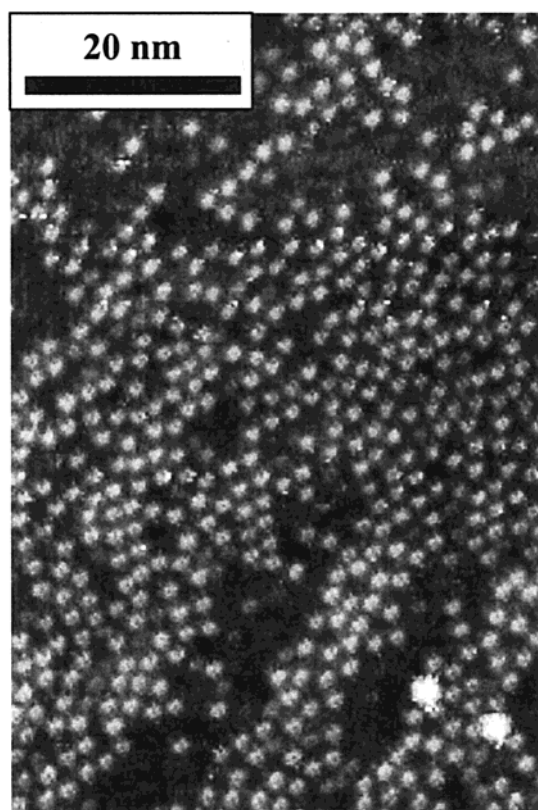


Figure 4. STM image of FePh in 0.1 M NaClO_4 . STM images of NiPh and ZnPh are very similar but with lower contrast.

10^{-4} M aqueous solution of each of the dye molecule into the SPR cell and monitored the SPR shift while the adsorption took place. The shift stopped within 30 min, corresponding to a maximum coverage of the adsorbed molecules. Replacing the molecule-containing solution in the SPR cell with blank electrolyte introduced no further change in the SPR angle, indicating that the adsorbed molecules were rather stable on the electrode. After reaching the maximum adsorption, we applied a potential modulation to the electrode and measured the potential modulation-induced SPR shift ($\Delta\theta/\Delta V$) as a function of λ . The result, as plotted in Figure 3 for NiPh, shows pronounced dips near 640

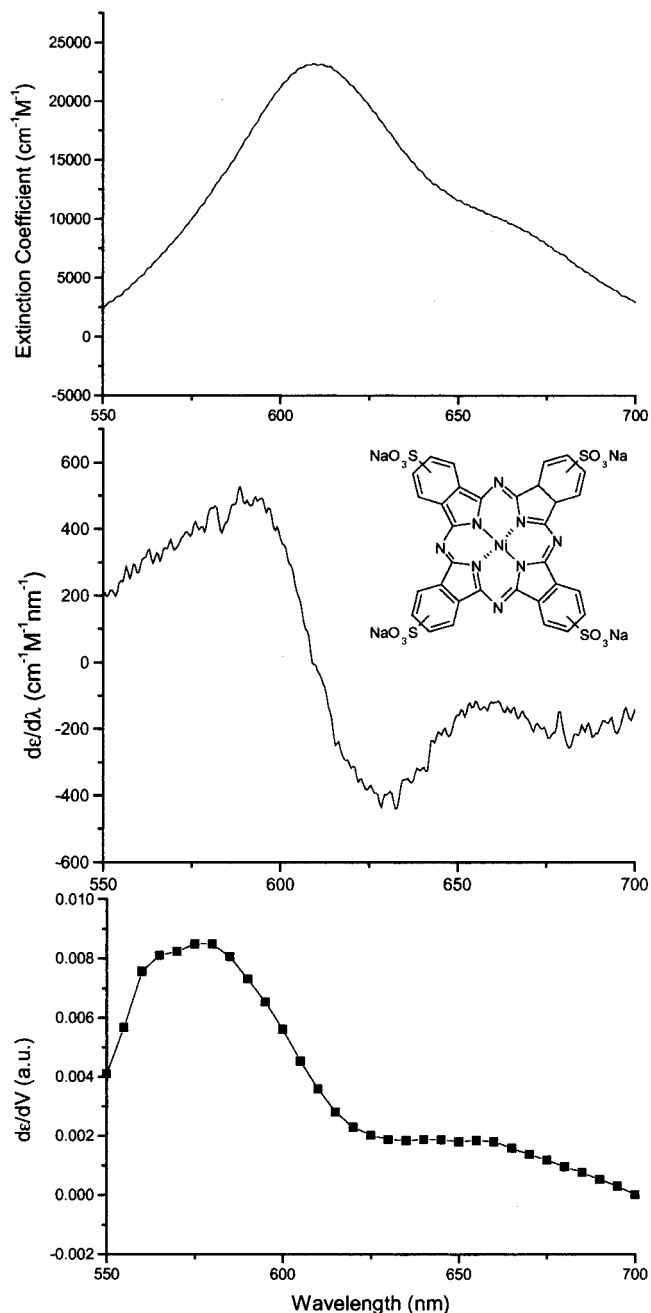


Figure 5. Top: solution-phase absorption spectrum of NiPh in 0.1 M NaClO_4 . Middle: derivative of the absorption spectrum. Bottom: Stark spectrum obtained from SPR angular shift and Kramers–Kronig relation.

nm. In sharp contrast, the plot for the thiol molecule, $\text{HOOC}(\text{CH}_2)_{10}\text{SH}$, shows a weak and smooth dependence on λ within the same wavelength range. The dip for NiPh is due to the Stark effect because no detectable electrochemical processes, such as reactions or desorption, take place upon a 20-mV potential modulation around 0.2 V. We have imaged the molecules with electrochemical STM over a large potential window and observed no changes in the adsorbed molecular layer (Figure 4).

By integrating $\Delta\theta(\lambda)/\Delta V$ shown in eq 2, we have extracted $\Delta\epsilon(\lambda)/\Delta V$ that is directly comparable to conventional Stark spectroscopy. Previous Stark spectroscopy studies¹ found that the applied electric field often induces a dipole moment in only one

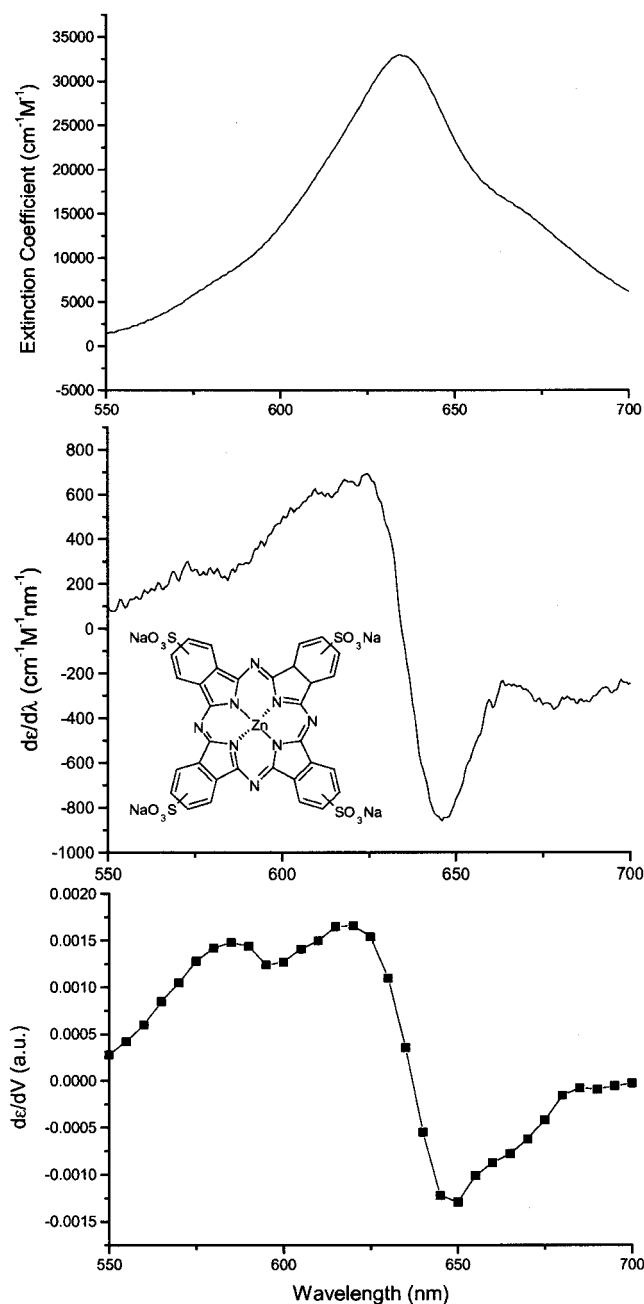


Figure 6. Top: solution-phase absorption spectrum of ZnPh in 0.1 M NaClO₄. Middle: derivative of the absorption spectrum. Bottom: Stark spectrum obtained from SPR angular shift and Kramers–Kronig relation.

direction, regardless of the molecular orientation, and the absorption shifts toward lower energy. Consequently, the field shifts the entire absorption spectrum to a higher or lower wavelength without changing its shape, and the Stark spectrum is given by the first-order derivative of the absorption spectrum with respect to the wavelength.

Figure 5 compares the Stark spectrum (bottom) obtained with the SPR method with the solution-phase absorption spectrum (top) and first derivative (middle) of the absorption spectrum of NiPh. The solution-phase absorption spectrum was measured using 10⁻⁴ M NiPh + 0.1 M NaClO₄, which shows a typical peak of phthalocyanine at ~610 nm. The first-order derivative of this spectrum shows a kink around 610 nm. The Stark spectrum is

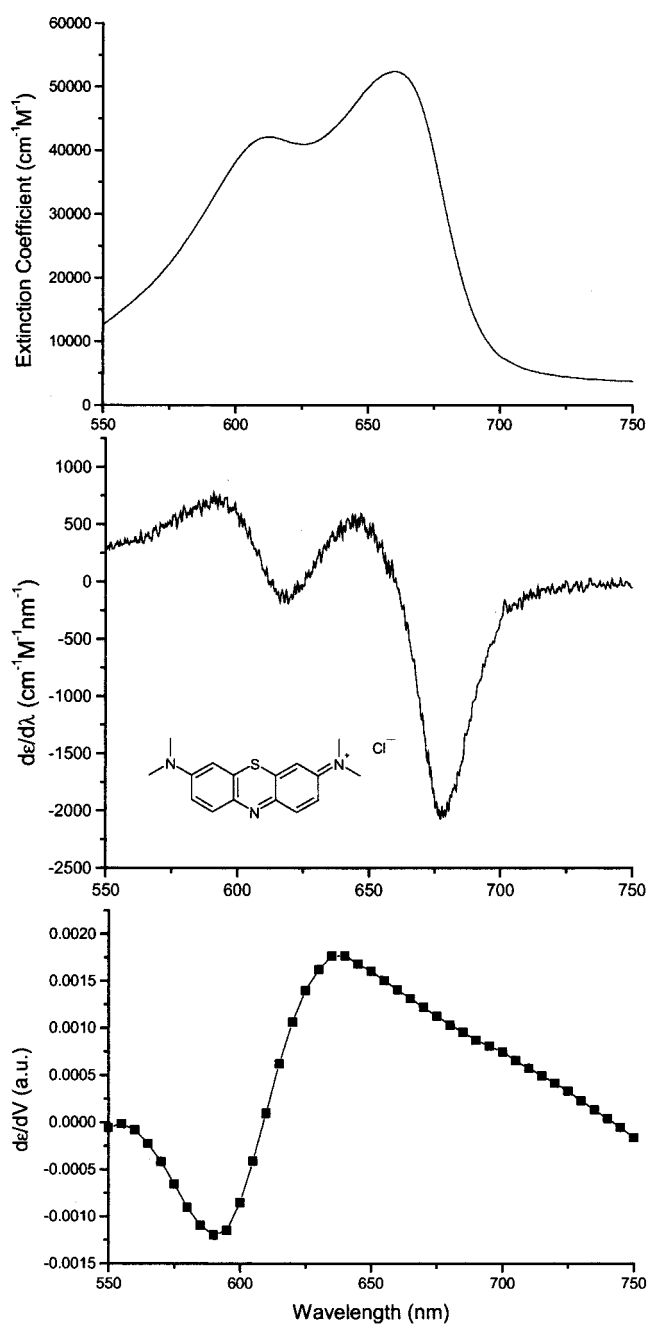


Figure 7. Top: solution-phase absorption spectrum of methylene blue in 100 mM phosphate buffer (pH 7) with 0.1 M NaClO₄. Middle: derivative of the absorption spectrum. Bottom: Stark spectrum obtained from SPR angular shift and Kramers–Kronig relation.

similar to the first derivative of the absorption spectrum, demonstrating that the electrode potential shifts absorption energy of the molecule.

We studied ZnPh in a way similar to NiPh and plotted the results in Figure 6. The solution-phase absorption spectrum (top) shows that the phthalocyanine peak is somewhat sharper and located at a longer wavelength (~635 nm) than NiPh. The corresponding first-order derivative (middle) of the absorption spectrum shows also a sharper kink. The Stark spectrum obtained from our SPR method is again similar to the first derivative of the absorption spectrum, including a sharper kink than that of NiPh.

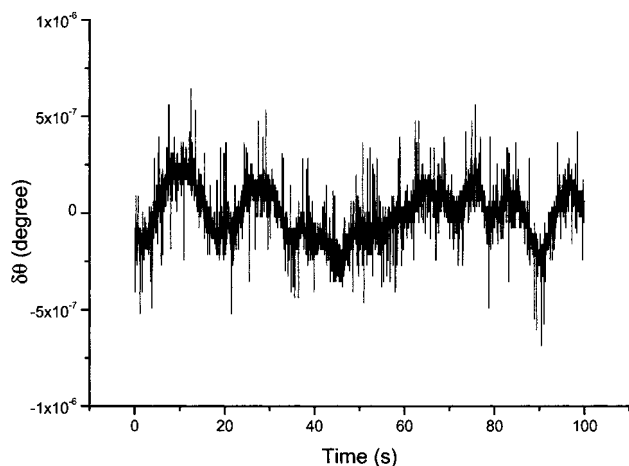


Figure 8. Angular resolution of potential-modulated SPR measurement. Sample, $\text{CH}_3(\text{CH}_2)_9\text{SH}$ in 0.1 M NaClO_4 ; potential modulation range, 200 ± 10 mV; frequency, 200 Hz; time constant of lock-in amplifier, 3 s; standard derivation, 1.3×10^{-7} deg.

The Stark spectra of both NiPh and ZnPh are similar to the first derivatives of the absorption spectra; the Stark spectrum of methylene blue, however, shows a totally different behavior (Figure 7, bottom). While the first-order derivative of the absorption spectrum has two kinks around 610 and 660 nm, respectively, the Stark spectrum shows a minimum at 590 nm and a maximum at 635 nm. This result is in good agreement with the electroreflectance spectrum of methylene blue on a pyrolytic graphite electrode,⁶ which has a maximum at 580 nm and a minimum at 660 nm. The departure of the Stark spectrum from the simple first derivative of the corresponding absorption spectrum suggests that the electric field does not simply induce a shift in the absorption spectrum in the case of methylene blue. As explained by Sagara and Niki,⁶ at a potential of 0.2 V, the surface-adsorbed methylene blue is in reduced form with an absorption peak around 580–630 nm (ER state II), which is different from the colorless solution of reduced methylene blue.

(27) Plieth, W. *Ber. Bunsen-Ges. Phys. Chem.* **1972**, 76, 485.

DISCUSSION

Different from the conventional Stark spectroscopy that measures intensity changes, the sensitivity of the present SPR-based method depends on the angular resolution of the SPR setup. Using our differential detection, we have achieved a resolution of 10^{-6} deg with the lock-in detection method (Figure 8). This angular sensitivity is estimated to be equivalent to a sensitivity of $\Delta R/R \sim 10^{-7}$ in the electroreflectance measurement, while a typical electroreflectance measurement reaches a sensitivity of 10^{-6} .²⁷ The present method allows one to monitor the kinetics of molecular adsorption onto electrode surfaces and to determine molecular coverage.

CONCLUSION

We have demonstrated a novel approach to obtain Stark spectroscopy of molecular adsorbates using high-resolution SPR spectroscopy. Using the approach, we have studied the Stark effect of several molecules by monitoring the SPR angular shift upon modulating the electrode potential as a function of wavelength. We have extracted the Stark spectra that are comparable to conventional Stark spectroscopy by the Kramers–Kronig relation. The Stark spectra of Ni(II)– and Zn–phthalocynine–tetrasulfonic acid tetrasodium salts are very similar to the first derivatives of their solution-phase absorption spectra, corresponding to a shift in the absorption peak upon the perturbation of electric field. The Stark spectrum of methylene blue, however, shows a more complicated behavior. In comparison to conventional electroreflectance measurement, the present method is highly sensitive and surface specific with the capability of studying adsorption kinetics as in a regular SPR.

ACKNOWLEDGMENT

Financial support is acknowledged through grants from NSF (CHE-9818073), NIH (GM-08205), and the donors of the Petroleum Research Fund (33516-AC5) administered by the ACS.

Received for review May 2, 2000. Accepted June 9, 2000.

AC000504F